Protected Quantum Computing: Interleaving Gate Operations with Dynamical Decoupling Sequences

Jingfu Zhang,[1] Alexandre M. Souza,[2] Frederico Dias Brandao,[1] and Dieter Suter[1]
[1]Fakultät Physik, Technische Universität Dortmund, D-44221 Dortmund, Germany
[2]Centro Brasileiro de Pesquisas Físicas, Rua Dr. Xavier Sigaud 150, Rio de Janeiro 22290-180, RJ, Brazil
(Received 19 July 2013; published 6 February 2014)

Implementing precise operations on quantum systems is one of the biggest challenges for building quantum devices in a noisy environment. Dynamical decoupling attenuates the destructive effect of the environmental noise, but so far, it has been used primarily in the context of quantum memories. Here, we experimentally demonstrate a general scheme for combining dynamical decoupling with quantum logical gate operations using the example of an electron-spin qubit of a single nitrogen-vacancy center in diamond. We achieve process fidelities $> 98\%$ for gate times that are 2 orders of magnitude longer than the unprotected dephasing time T_2.

DOI: 10.1103/PhysRevLett.112.050502 PACS numbers: 03.67.Lx, 33.35.+r, 76.70.-r

Realizing the potential of quantum computation [1,2] hinges on the implementation of fault-tolerant systems that complete the computational process with high fidelity even in the presence of unavoidable environmental perturbations. Quantum error correction offers this possibility, at the cost of an overhead in the number of qubits, provided that the error per gate can be kept sufficiently low [3] and the preparation of the initial states is achieved with sufficiently high fidelity [4,5]. Achieving these goals requires additional techniques for eliminating the effect of perturbations both between and inside the quantum operations. Ideally, these additional measures should require little or no additional resources.

Dynamical decoupling (DD) is an attractive approach for protecting the qubit system against unwanted environmental interactions, which may be static or time dependent. It relies on a sequence of control operations applied to the system, which refocuses the system-environment interaction. It does not require additional qubits, and DD sequences can be designed such that they work reliably even in the presence of unavoidable experimental imperfections [6–9]. Experimental tests of DD have demonstrated this potential by reducing decoherence rates in different systems by several orders of magnitude [7,10–15].

While most of these tests demonstrated the protection of single qubits in quantum memories, environmental noise also degrades the fidelity of quantum gate operations during computational processes [16]. If the relaxation mechanism is known, it is possible to design protected quantum gates by optimal control techniques [17]. If the environment is not characterized, it may be still possible to use DD techniques for protecting quantum gate operations. In the simplest case, quantum operations can be made robust against static noise by refocusing them in a way similar to a Hahn echo [18]. In the case of a general fluctuating environment, the Hahn echo must be replaced by DD methods. Initial experiments demonstrating decoherence protected quantum gates have been made recently on nitrogen-vacancy (NV) centers [19], semiconductor quantum dots [20], and solid-state nuclear spins [16].

Possible approaches to build DD protected gates were proposed by several groups [16,21–27]. The simplest way to combine DD and gate operations consists of applying the operations between two consecutive DD cycles. It was theoretically shown that this approach can lower the resource requirements for quantum error correction [24]. However, if the duration of a single gate operation is comparable to or longer than the decoherence time of the system, this approach will fail. It then becomes necessary to apply protection schemes in parallel to the gate operation. This must be done in such a way that the DD, which is designed to eliminate the effect of interactions with the environment, does not eliminate the interaction between the qubits and the control fields driving the gate operation [21].

In this Letter, we demonstrate how it is possible to modify general logical gate operations in such a way that they can be interleaved with DD sequences without using auxiliary or encoded qubits. Our method removes the system-environment interaction for any gate operation at least to first order and it allows one to combine arbitrary DD sequences with any type of quantum gate operation.

We consider a system governed by the Hamiltonian

$$\mathcal{H}(t) = \mathcal{H}_s + \mathcal{H}_c(t) + \mathcal{H}_{se} + \mathcal{H}_e, \tag{1}$$

where $\mathcal{H}_s$ describes the internal Hamiltonian of the qubit, $\mathcal{H}_c(t)$ is a time-dependent control Hamiltonian driving the logical gates, $\mathcal{H}_{se}$ is the interaction of the qubit with the environment, and $\mathcal{H}_e$ describes the evolution of the environmental degrees of freedom. Our goal is to implement gate operations protected against environmental

 © 2014 American Physical Society

noise. Our target operation is a unitary gate $U_t = U_g \otimes \mathcal{T} e^{-i\int_0^\tau \mathcal{H}_e dt}$ that is not affected by the system-environment interaction $\mathcal{H}_{se}$. Here, the gate operation U_g is a pure system operator, $\mathcal{T}$ is the Dyson time ordering operator, and τ is the duration of the gate operation.

Protecting the system from the environmental noise while simultaneously driving logical gate operations can be achieved by using a standard DD sequence and inserting a suitably adapted gate operation in short increments in the free precession periods of the DD sequence. Figure 1 illustrates this for the $XY-4$ DD sequence: in the free precession periods between the DD pulses, we insert a control Hamiltonian $\mathcal{H}_n = \mathcal{H}_s + \mathcal{H}_{c,n} + \mathcal{H}_{se} + \mathcal{H}_e$, where $(n = 1, \ldots, 5)$ indicates the period for which this Hamiltonian is active. The evolution of the system can then be written as

$$U = U_{N+1} P_N U_N \cdots P_1 U_1 = U_{N+1} \Pi_{n=1}^{N} (P_n U_n), \quad (2)$$

where N is the number of pulses of the DD sequence ($N = 4$ in the case of $XY-4$), $P_n = e^{-i\pi I_\alpha}$ is the propagator describing the nth DD inversion pulse, I_α is the Cartesian component of the spin operator, and $U_n = e^{-i\mathcal{H}_n \tau_n}$ is the evolution between two DD pulses. We assume that these periods are short and the control Hamiltonians are time independent within each period. We treat the DD pulses P_n as ideal rotations.

To find the required control Hamiltonians $\mathcal{H}_n$, we rewrite Eq. (2) in the form

$$U = U_{N+1} \Pi_{n=1}^{N} \tilde{U}_n = U_{N+1} \Pi_{n=1}^{N} e^{-i\tilde{H}_n \tau_n}, \quad (3)$$

where the Hamiltonian $\tilde{\mathcal{H}}_n = T_n^{-1} \mathcal{H}_n T_n$ describe the control fields in the so-called toggling frame [28] of the DD sequence, which are defined by the transformations $T_n = P_{n-1} P_{n-2} \cdots P_1$, and include the limiting cases $T_1 = T_{N+1} = E$ (identity). This approach guarantees first order protection of any operation interlaced with a suitable dynamical decoupling sequence. A brief proof is presented in the Supplemental Material (SM) [29]

As a specific example, we choose the $XY-4$ and $XY-8$ DD sequences to protect the gate operations NOOP (no operation, i.e., identity), NOT, Hadamard, and phase gate, which can be represented as

$$\begin{pmatrix} 1 & 0 \\ 0 & 1 \end{pmatrix}, \quad \begin{pmatrix} 0 & 1 \\ 1 & 0 \end{pmatrix}, \quad \frac{1}{\sqrt{2}} \begin{pmatrix} 1 & 1 \\ 1 & -1 \end{pmatrix}, \quad \begin{pmatrix} 1 & 0 \\ 0 & i \end{pmatrix}. \quad (4)$$

To protect these gates, we first split them up into segments that can be interleaved with the DD sequence. A possible decomposition is

$$\begin{aligned} \text{NOT}&: (\pi/8)_0 - (\pi/4)_0 - (\pi/4)_0 - (\pi/4)_0 - (\pi/8)_0, \\ \boldsymbol{H}&: (\pi/4)_{3\pi/2} - (\pi/2)_0 - (0)_0 - (\pi/2)_0 - (\pi/4)_{\pi/2}, \\ \text{phase}&: (0)_0 - (\pi/2)_0 - (\pi/2)_{\pi/2} - (\pi/2)_0 - (0)_0, \end{aligned} \quad (5)$$

with time running from left to right. Here, $(\theta)_\phi = e^{-i\theta(I_x \cos\phi - I_y \sin\phi)}$ denotes a pulse with flip angle θ and phase ϕ. The short line between the pulses denotes a variable delay for adjusting the overall gate duration. $(0)_0$ denotes a "pulse" with zero amplitude but nonzero duration for balancing the delays in the DD sequence: the duration of $(0)_0$ in the Hadamard gate, e.g., is the same as that of the $(\pi/2)$ pulse. The decomposition of the gates is not unique, as discussed in the SM [29]. Here, we choose a decomposition that is sufficiently symmetric to eliminate odd order terms in the Magnus expansion [29–31]. The transformation into the toggling frame changes the phases to $0-0-\pi-\pi-0$, $3\pi/2-0-0-\pi-\pi/2$, and $0-\pi-\pi/2-\pi-0$ for the NOT, Hadamard, and phase gates, respectively.

The lower part of Fig. 2 shows the resulting sequence, combining the gate operation and the DD cycle, together with the first pulse that generates the initial condition and the last pulse as the readout pulse of the quantum-state tomography. In the experiments, we adjust the overall gate duration τ_c by changing the delays τ between the pulses while keeping the power of the microwave (MW) pulses constant. While we have discussed the example of the $XY-4$ sequence, the scheme is equally applicable to other

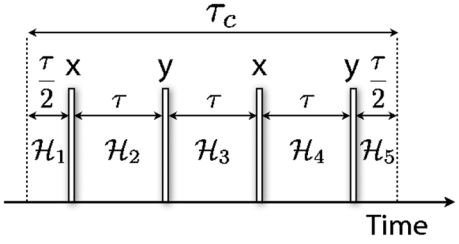

FIG. 1. Single cycle of an $XY-4$ DD sequence used as the basis of protected gate operations. The labels x and y mark the rotation axes of the DD pulses, and $\mathcal{H}_n$ is the Hamiltonian between the DD pulses.

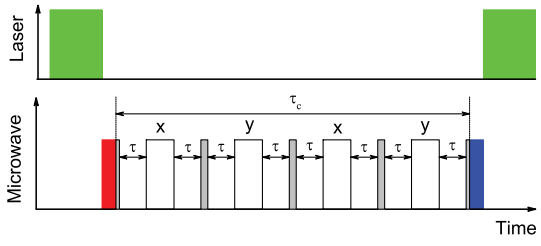

FIG. 2 (color online). Laser (top) and microwave (bottom) pulse sequences for the NOT gate protected by an $XY-4$ DD cycle. The duration of the laser pulses is 400 ns. The pulse sequence (duration τ_c) between the first and last pulses implements the protected NOT gate, where unfilled boxes represent the DD pulses and filled ones represent the segments of the gate operation.

DD schemes. As additional tests, we have experimentally implemented gates protected by the $XY-8$ DD sequence, using the sequences shown in the SM [29].

For the experimental test, we used the NV center of the diamond [32], which has an electronic spin $S=1$. The SM [29] contains a description of the experimental setup. We apply a magnetic field along the NV symmetry axis to lift the degeneracy of the $m_S=\pm 1$ states and use the subsystem consisting of the $m_s=0$ and $+1$ states as a single qubit. In the secular approximation, we can write an effective Hamiltonian for the two-level system as

$$H_{\mathrm{NV}} = \omega_S S_z + S_z \sum_j A_j I_z^j + \sum_j \omega_I I_z^j + H_{\mathrm{dip}} = \mathcal{H}_s + \mathcal{H}_{se} + \mathcal{H}_e. \quad (6)$$

Here, S_z and I_z^j denote the electron- and nuclear-spin operators, ω_S and ω_I their resonance frequencies, A_j the hyperfine coupling between the electron and the jth nuclear spin, and H_{dip} the dipolar coupling within the nuclear-spin bath that generates the environmental noise.

Figure 2 illustrates the pulse sequence for implementing a NOT gate protected by an $XY-4$ cycle and measuring the performance. The first laser pulse initializes the spin into state $|0\rangle$. The second laser pulse implements the measurement of the population of state $|0\rangle$. The MW pulse sequence is applied between the two laser pulses. The first MW pulse initializes the state $|0\rangle$ into the input state required for the process tomography, and the last pulse implements the required readout.

For a quantitative evaluation of the effectiveness of our scheme, we used quantum process tomography [22] to describe the process as $\rho_{\mathrm{out}} = \sum_{kl} \chi_{kl} e_k \rho_{\mathrm{in}} e_l^\dagger$, where the basis operators are $e_{k,l} \in \{E, X, iY, Z\}$ and X, Y, and Z represent Pauli operators. For each protected gate, we prepared four states $|0\rangle$, $|1\rangle$, $(|0\rangle+|1\rangle)/\sqrt{2}$, and $(|0\rangle - i|1\rangle)/\sqrt{2}$ as the input states. To analyze the output states, we used quantum-state tomography, which requires four readout operations. Here, we used E, $(\pi/2)_0$, $(\pi/2)_{\pi/2}$, and $(\pi)_0$. The procedure is described in the SM [29]. Figure 3 shows the measured χ matrices for all four gate operations protected by the $XY-8$ sequence, each for a gate duration of ≈ 35.5 μs. For the first three gates, where the χ matrices of the ideal gates are real, we only show the real part. The imaginary parts have rms values of 0.013, 0.016, and 0.027, respectively.

These matrices prove that the experimentally implemented gates agree well with the targeted gate operation. We thus conclude that our method of interleaving gate operations with DD sequences works and avoids destructive interference between the gate operation and the DD sequence.

To compare the efficiency of the protection schemes quantitatively, we determined the gate fidelity from the χ matrices as [33]

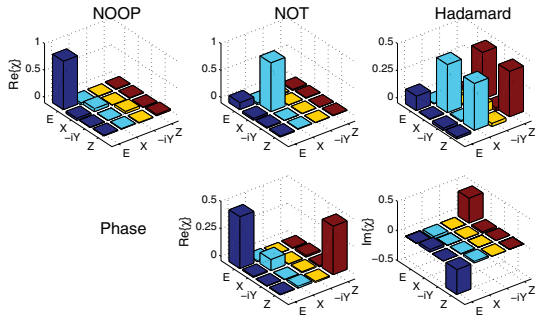

FIG. 3 (color online). χ matrices measured by quantum process tomography for the NOOP, NOT, Hadamard, and phase gates protected by $XY-8$ dynamical decoupling pulses, for gate durations of ≈ 35.5 μs. The first row shows the real parts of the NOOP, NOT, and Hadamard gates, and the second row shows real and imaginary parts of the phase gate. The imaginary parts for the NOOP, NOT, and Hadamard gates are not shown; their rms values are < 0.03, which is compatible with zero within experimental uncertainties.

$$F_\chi = |Tr(\chi_{exp}\chi_{th}^\dagger)| \Big/ \sqrt{Tr(\chi_{exp}\chi_{exp}^\dagger) Tr(\chi_{th}\chi_{th}^\dagger)}, \quad (7)$$

where χ_{th} and χ_{exp} denote the theoretical and experimental χ matrices, respectively. For the χ matrices represented in Fig. 3, the measured gate fidelities are 0.993, 0.985, 0.975, and 0.989 for the protected NOOP, NOT, Hadamard, and phase gates. In Fig. 4, we show how the gate fidelity changes with increasing gate duration. While the fidelity of the unprotected gates drops sharply on a time scale of ≈ 0.2 μs, the protected gates retain fidelities of $\approx 99\%$ for up to 80 μs—clearly demonstrating that the protection against environmental noise also works well for the gate operations.

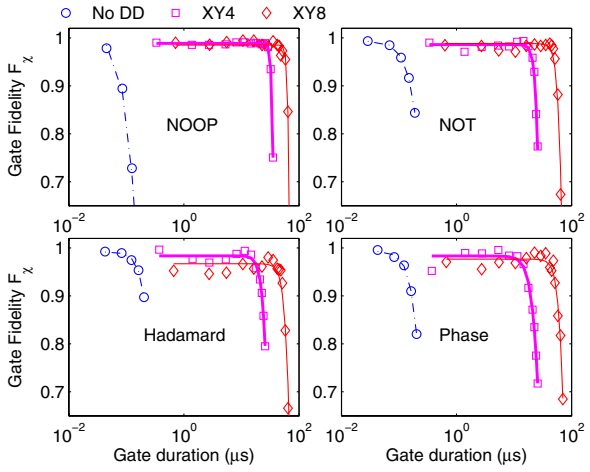

FIG. 4 (color online). The measured gate fidelity obtained by quantum process tomography for the gates without and with dynamical decoupling pulses. The curves are functions $Ae^{-(t/T_2)^k}$, with the fit parameters of Table III in the SM.

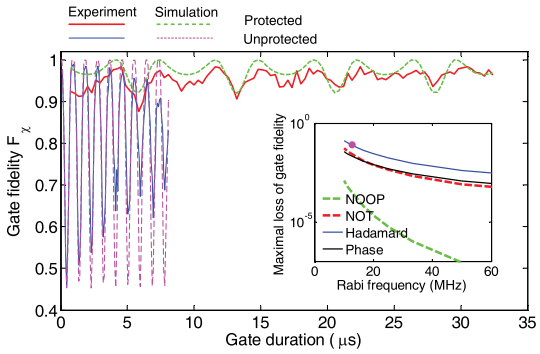

FIG. 5 (color online). Effect of the hyperfine coupling between the electron and the ^{14}N nuclear spin on the fidelity of the Hadamard gate. The measured fidelity of the gate protected by an $XY-8$ cycle is shown as the solid thick curve and the simulated fidelity for the same gate as the dashed thick curve. The dashed thin curve shows the fidelity of the unprotected gate by simulation and the solid thin curve the corresponding experimental data. The inset shows how the maximal loss of the gate fidelity decreases with increasing Rabi frequency of the control pulses according to the simulation. The point on the solid thick curve, at a Rabi frequency of 12.7 MHz, indicates the value corresponding to the main plot.

For a quantitative evaluation, we fitted the experimental data with the function $Ae^{-(t/T_2)^k}$ [7,34]. The parameters obtained from this fit are listed in Table III in the SM [29]. Within experimental uncertainty, the amplitude A is very close to 1.0 for all gates. The most important parameter for assessing the effectiveness of the scheme is the decay time T_2 of the gate fidelity. Compared to the unprotected gates, the gates protected by $XY-4$ extend this lifetime by factors of 201, 83, 89, and 103 for NOOP, NOT, Hadamard, and phase gates, respectively, and the $XY-8$ scheme achieves factors of 375, 210, 212, and 258.

The decay of the gate fidelity in the NV center is dominated by the hyperfine interaction with the ^{13}C nuclear spins, which are present at 1.1% of the sites in diamond (natural abundance). In addition, the electron spin is also coupled to the ^{14}N nuclear spin ($I=1$) of the NV center, through a hyperfine interaction of $A_{^{14}N} \approx 2\pi \times 2.15$ MHz. In contrast to the nuclear-spin bath, this single spin represents a time-independent perturbation, which also affects the gate performance, and the coupling strength is significantly larger than that of the ^{13}C nuclear spins. In the data shown in Fig. 4, we eliminated its effect by an appropriate choice of the delays between the pulses. In Fig. 5, we explicitly show its effect for the example of the Hadamard gate. The data shown here correspond to the data represented in the lower left panel of Fig. 4, but with higher resolution and using a linear scale. The oscillations visible in the experimental as well as the simulated data are due to the hyperfine interaction with the ^{14}N nuclear spin. The damping of the experimental oscillations, which is not visible in the simulated data, can be attributed to the interaction with the ^{13}C nuclear-spin bath, which was not considered in the simulations. Clearly, the protection scheme is also helpful for this type of interaction. In the inset of the figure, we show how this effect can be eliminated by increasing the Rabi frequency of the control pulses. Alternatively, DD pulses that are robust against off-resonance errors should further suppress this effect [7].

Some single-qubit gates, such as a population transfer, can be effectively implemented through adiabatic pulses [35–37]. In this approach, one component of a quantum state can be locked by the control field. This locking is robust against amplitude errors of the control field, but the components orthogonal to the field are dephased. Adiabatic gates are therefore not suitable for preserving unknown quantum states, an important requirement for quantum information processing.

The scheme outlined here should be useful for improving the gate fidelity in various cases. Examples include the following. (i) In most cases, where the gate fidelity is dominated by environmental noise, it should be possible to design protected gates that provide better overall fidelity. We have demonstrated this in our previous work using solid-state NMR [16] with a simpler scheme. The present scheme leads to shorter gates and better protection. (ii) In implementing quantum computing, many quantum algorithms require the application of single-qubit gate operations to several qubits. Generally, it will be advantageous to apply them in parallel, to reduce the overall duration of the algorithm. In either case, it will be necessary to synchronize the gates. If one of the gate operations is applied to a "slow" qubit, e.g., to a nuclear spin that has a significantly lower gyromagnetic ratio than an electron spin in the NV center system, it is important to protect the gate for the "fast" electron spin, to prevent it from dephasing. (iii) In the case of two-qubit gates, the synchronization is, of course, essential. Again, the typical example here will be a multiqubit quantum register that includes different types of qubits, e.g., electronic and nuclear spins [38,39]. Even in the case of a single type of qubit (e.g., only nuclear spins [40]), the duration of a two-qubit gate is determined by the interaction strength and it cannot be accelerated by increasing the strength of the control field.

In conclusion, we have implemented a scheme for protecting quantum logical gate operations against environmental noise by segmenting the gate operations and interleaving them with a pulse cycle for dynamical decoupling. The interleaving process requires that the segments of the gate operations be modified in such a way that the DD pulses effectively transform them into the operations required by the algorithm. In the experimental example, using the NV center of diamond, we demonstrated that protected gates retain high fidelity for durations that are more than 2 orders of magnitude longer than for unprotected gates. In future work, we plan to extend this work to

other DD sequences and to multiqubit systems. In the SM [29], we outline how the scheme presented here can be applied to two-qubit gates. Numerical simulations show that this should allow us to effectively suppress environmental noise.

We gratefully acknowledge experimental assistance from J. H. Shim and useful discussions with L. Viola, G. A. Álvarez, and J. Filgueiras. This work was supported by the DFG through Grant No. Su 192/27-1. A. M. S. acknowledges the Brazilian National Institute for Science and Technology of Quantum Information (INCT-IQ).

[1] M. A. Nielsen and I. L. Chuang, *Quantum Computation and Quantum Information* (Cambridge University Press, Cambridge, England, 2000).
[2] J. Stolze and D. Suter, *Quantum Computing: A Short Course from Theory to Experiment* (Wiley-VCH, Berlin, 2008), 2nd ed.
[3] E. Knill, R. Laflamme, and W. H. Zurek, Science **279**, 342 (1998).
[4] S. Bravyi and A. Kitaev, Phys. Rev. A **71**, 022316 (2005).
[5] A. M. Souza, J. Zhang, C. A. Ryan, and R. Laflamme, Nat. Commun. **2**, 169 (2011).
[6] T. Gullion, D. B. Baker, and M. S. Conradi, J. Magn. Reson. **89**, 479 (1990).
[7] C. A. Ryan, J. S. Hodges, and D. G. Cory, Phys. Rev. Lett. **105**, 200402 (2010).
[8] A. M. Souza, G. A. Álvarez, and D. Suter, Phil. Trans. R. Soc. A **370**, 4748 (2012).
[9] M. A. Ali Ahmed, G. A. Álvarez, and D. Suter, Phys. Rev. A **87**, 042309 (2013).
[10] M. J. Biercuk, H. Uys, A. P. VanDevender, N. Shiga, W. M. Itano, and J. J. Bollinger, Nature (London) **458**, 996 (2009).
[11] J. Du, X. Rong, N. Zhao, Y. Wang, J. Yang, and R. B. Liu, Nature (London) **461**, 1265 (2009).
[12] G. A. Álvarez, A. Ajoy, X. Peng, and D. Suter, Phys. Rev. A **82**, 042306 (2010).
[13] G. deLange, Z. H. Wang, D. Risté, V. V. Dobrovitski, and R. Hanson, Science **330**, 60 (2010).
[14] A. M. Souza, G. A.Álvarez, and D. Suter, Phys. Rev. Lett. **106**, 240501 (2011).
[15] A. Ajoy, G. A. Álvarez, and D. Suter, Phys. Rev. A **83**, 032303 (2011).
[16] A. M. Souza, G. A. Álvarez, and D. Suter, Phys. Rev. A **86**, 050301 (2012).
[17] T. Schulte-Herbruggen, A. Sporl, N. Khaneja, and S. J. Glaser, J. Phys. B **44**, 154013 (2011).
[18] M. D. Shulman, O. E. Dial, S. P. Harvey, H. Bluhm, V. Umansky, and A. Yacoby, Science **336**, 202 (2012).
[19] T. van der Sar, Z. H. Wang, M. S. Blok, H. Bernien, T. H. Taminiau, D. M. Toyli, D. A. Lidar, D. D. Awschalom, R. Hanson, and V. V. Dobrovitski, Nature (London) **484**, 82 (2012).
[20] C. Barthel, J. Medford, C. M. Marcus, M. P. Hanson, and A. C. Gossard, Phys. Rev. Lett. **105**, 266808 (2010).
[21] L. Viola, S. Lloyd, and E. Knill, Phys. Rev. Lett. **83**, 4888 (1999).
[22] K. Khodjasteh and L. Viola, Phys. Rev. Lett. **102**, 080501 (2009).
[23] K. Khodjasteh, D. A. Lidar, and L. Viola, Phys. Rev. Lett. **104**, 090501 (2010).
[24] J. R. West, D. A. Lidar, B. H. Fong, and M. F. Gyure, Phys. Rev. Lett. **105**, 230503 (2010).
[25] K. Khodjasteh and L. Viola, Phys. Rev. A **80**, 032314 (2009).
[26] H.-K. Ng, D. A. Lidar, and J. Preskill, Phys. Rev. A **84**, 012305 (2011).
[27] P. Cappellaro, L. Jiang, J. S. Hodges, and M. D. Lukin, Phys. Rev. Lett. **102**, 210502 (2009).
[28] U. Haeberlen, in *Advances in Magnetic Resonance*, edited by J. Waugh (Academic, New York, 1976), Supplement 1.
[29] See Supplemental Material at http://link.aps.org/supplemental/10.1103/PhysRevLett.112.050502 for details on (1) a protected two-qubit gate, (2) the normalization of the quantum process tomography, (3) proof of first order protection, (4) different decompositions for the protected Hadamard gate, (5) a description of the experimental setup, and (6) other parameters used in the experiment and obtained in data analysis.
[30] D. P. Burum, Phys. Rev. B **24**, 3684 (1981).
[31] A. M. Souza, G. A. Álvarez, and D. Suter, Phys. Rev. A **85**, 032306 (2012).
[32] J. Wrachtrup and F. Jelezko, J. Phys. Condens. Matter **18**, S807 (2006).
[33] X. Wang, C.-S. Yu, and X. Yi, Phys. Lett. **373A**, 58 (2008).
[34] J. Shim, I. Niemeyer, J. Zhang, and D. Suter, Europhys. Lett. **99**, 40004 (2012).
[35] X. Lacour, S. Guérin, N. V. Vitanov, L. P. Yatsenko, and H. R. Jauslin, Opt. Commun. **264**, 362 (2006).
[36] M. Andrecut and M. K. Ali, J. Phys. A **37**, L267 (2004).
[37] N. V. Vitanov and B. W. Shore, Phys. Rev. A **73**, 053402 (2006).
[38] J. S. Hodges, J. C. Yang, C. Ramanathan, and D. G. Cory, Phys. Rev. A **78**, 010303 (2008).
[39] Y. Zhang, C. A. Ryan, R. Laflamme, and J. Baugh, Phys. Rev. Lett. **107**, 170503 (2011).
[40] L. M. K. Vandersypen and I. L. Chuang, Rev. Mod. Phys. **76**, 1037 (2005).